Analysis of nocturnal air temperature in districts using mobile measurements and a cooling indicator

F Leconte, Julien Bouyer, Remy Claverie, Mathieu Pétrissans

Noname manuscript No.
(will be inserted by the editor)

Analysis of nocturnal air temperature in districts using mobile measurements and a cooling indicator

François Leconte · Julien Bouyer · Rémy Claverie · Mathieu Pétrissans

the date of receipt and acceptance should be inserted later

Abstract The urban heat island phenomenon is generally defined as an air temperature difference between a city center and the non-urbanized rural areas nearby. However, this description does not encompass the intra-urban temperature differences that exist between neighborhoods in a city. This study investigates the air temperature dynamics of neighborhoods for meteorological conditions that lead to important urban heat island amplitude. Local Climate Zones (LCZ) have been determined in Nancy, France, and mobile screen-height air temperature measurements are performed using an instrumented vehicle. Initially, hourly measurements are performed within four different LCZ. These results show that air temperature within LCZ demonstrates a nocturnal cooling in two phases, i.e. a first phase between 1 to 3 h before sunset and 3 to 5 h after sunset and a second phase from 3 to 5 h after sunset to sunrise. During phase 1, neighborhoods exhibit different cooling rate values and air temperature gaps develop between districts, while during phase 2, cooling rates tend to be analogous. Then, a larger meteorological data set is used to investigate these two phases for a selection of 13 LCZ. Normalized cooling rate are calculated between daytime measures and nighttime measures in order to quantify the air temperature dynamics of the studied areas during phase 1. Considering this indicator, three groups are emerging :

François Leconte
ADEME, 20 Avenue du Grésillé, BP 90406, 49004 Angers Cedex 01, France
CEREMA Direction Territoriale Est, 71 Rue de la Grande Haie, 54510 Tomblaine, France
LERMAB, Boulevard des Aiguillettes, BP 70239, 54506 Vandoeuvre les Nancy Cedex, France
Tel.: +33 3 83 18 41 41
E-mail: francois.leconte@cerema.fr

Julien Bouyer
CEREMA Direction Territoriale Est, 71 Rue de la Grande Haie, 54510 Tomblaine, France
E-mail: julien.bouyer@cerema.fr

Rémy Claverie
CEREMA Direction Territoriale Est, 71 Rue de la Grande Haie, 54510 Tomblaine, France
E-mail: remy.claverie@cerema.fr

Mathieu Pétrissans
LERMAB, Boulevard des Aiguillettes, BP 70239, 54506 Vandoeuvre les Nancy Cedex, France
E-mail: mathieu.petrissans@univ-lorraine.fr

- LCZ Compact Midrise and Open Midrise with mean normalized cooling rates values of 0.09 h^{-1}
- LCZ Large Lowrise and Open Lowrise/Sparsely Built with mean normalized cooling rates values of 0.011 h^{-1}
- LCZ Low Plants with mean normalized cooling rates values of 0.014 h^{-1}

Results indicate that the relative position of LCZ within the conurbation does not drive air temperature dynamics during phase 1. In addition, measures performed during phase 2 tend to illustrate that cooling rates are similar for all LCZ during this period.

Keywords Cooling rate · Intra-urban temperature · Local Climate Zone · Mobile Measurements · Urban Indicators · Urban Heat Island

1 Introduction

Cities and regional governments are encouraged to take into account local climate for urban planning operations. Therefore, these authorities aim to increase their knowledge about the climate characteristics of their territories. This effort concerns namely the climatic description of various types of urban areas and the investigation of the urban heat island (UHI) phenomenon. The latter is an urban-induced climate feature that demonstrates a maximum amplitude under specific meteorological conditions, namely anticyclonic conditions with low wind speed and low cloud cover (Gartland, 2008).

Terrain classifications have been proposed in order to enhance general understanding of urban climate and to study the existing relationship between urban environment and urban climate. The local climate zone scheme (LCZ) (Stewart and Oke, 2012) is considered as the latest version of a group of urban classification schemes for climate studies. This categorization has been inspired by previous works, i.e. urban terrain zone (Ellefsen, 1990/1991) and urban climate zone (Oke, 2006). Its initial goal was to provide methodological support for urban meteorology campaigns. It has been utilized then for numerous other purposes, namely to structure the observations and interpret the results of UHI study (Alexander and Mills, 2014), design an urban monitoring network (Lelovics et al., 2014), analyze long term meteorological data sets (Fenner et al., 2014) (Emmanuel and Krüger, 2012), used as input data for physical model (Alexander et al., 2015). Moreover, in order to counterbalance the lack of relevant information about urban areas for climate studies, LCZ scheme aims to be applied worldwide in the following years (Bechtel et al., 2015). It appears that LCZ approach demonstrates a great potential regarding the investigation of the climate of a conurbation, notably for the study of the diurnal cycle of the UHI.

Regarding this latter issue, it appears that UHI amplitude – which is generally defined as the air temperature difference between an urban area and its rural area nearby – is low during daytime and significant during nighttime for mid-latitude cities during summertime (Erell et al., 2011). The UHI amplitude can also be negative in the early morning (Theeuwes et al., 2015). Over a diurnal cycle, UHI amplitude develops from a local minimum in the afternoon to a local maximum around 3 to 5 h after sunset. Oke (1987) explains that urbanized and dense areas cool down slower than non-urbanized, rural areas, mainly because of

their differences in terms of morphology, land use, material and anthropogenic heat release. Dynamical characteristics of UHI intensity can be investigated by calculating the evolution of air temperature over time, i.e. a heating rate or a cooling rate (e.g. (Upmanis et al., 1998) (Haeger-Eugensson and Holmer, 1999) (Runnalls and Oke, 2000) (Lee and Baik, 2010)), which can be written as:

$$\chi = \frac{\partial T_{air}}{\partial t} \tag{1}$$

Holmer et al. (2007) studied in Göteborg the nocturnal cooling of different urbanized areas. The analysis of the cooling rates calculated over a year of field measurements shows that urban cooling can be divided into two phases:

- A first phase, between 1 to 3 h before sunset and 3 to 5 h after sunset, when cooling rates differ between urban zones.
- A second phase, from 3 to 5 h after sunset to sunrise, when cooling rate are similar between urban zones.

Explanatory elements are provided by Holmer et al. (2007) to interpret this phenomenon. The first phase starts with unstable urban boundary layer and finishes when stable conditions are almost reached. The cooling process is dominated by the sensible heat release from the surface and by the long-wave radiative divergence. The local features of the neighborhoods – such as their morphology or their land use – have a strong influence on the temperature decrease. The second phase starts under stable conditions when an inversion has developed in the urban boundary layer. At this point, the cooling depends on the radiative properties of the air layer above the urban canopy, and the urban characteristics are no longer decisive. This two-phases cooling has been then observed in several studies for different climates, namely in Singapore (Chow and Roth, 2006), Adelaide, Australia (Erell and Williamson, 2007), Athens, Greece (Giannopoulou et al., 2010) and Ouagadougou, Burkina Faso (Holmer et al., 2013).

The necessity to analyze the cooling rate in different parts of the city has been previously underlined (Holmer et al., 2007). Therefore, this paper aims to describe and quantify the nocturnal cooling dynamics of various neighborhoods types. In order to characterize the urban areas, the LCZ scheme has been applied as this classification allows a detailed description of an urban form, taking into account both its morphology and its land use. The study tackles the diurnal temperature cycle with a focus on the cooling period when air temperature differences appears between neighborhoods and UHI amplitude develops. So as to examine field data, cooling rates are used accordingly to the method proposed by Holmer et al. (2007). This work presents cooling rate values that have been calculated based on mobile traverses in order to reach a high spatial density measures within numerous LCZ types. This study was carried out in the conurbation of Nancy, France during summer 2013.

2 Material and methods

2.1 Site description and LCZ determining process

Measurements have been performed in Nancy, a city located north east of France within the Lorraine region. This conurbation numbers approximately 286,000 in-

LCZ code	SVF (-)	AR (-)	H (m)	R (-)	Builti (%)	Imper (%)	Per (%)	LCZ type (-)
OUE	0.53	1.00	15.7	7	40	42	18	2 (Compact Midrise)
CEN	0.58	0.95	16.8	7	49	41	10	2 (Compact Midrise)
TRM	0.55	0.88	15.3	7	38	38	24	2 (Compact Midrise)
NAT	0.66	0.32	16.5	7	18	52	30	5 (Open Midrise)
THL	0.64	0.54	13.4	7	28	26	46	5 (Open Midrise)
SMA	0.66	0.51	11.0	7	28	42	30	5 (Open Midrise)
MBR	0.82	0.16	8.8	6	27	53	20	8 (Large Lowrise)
PVE	0.83	0.11	6.0	6	24	51	25	8 (Large Lowrise)
JAR	0.75	0.20	4.8	5	22	18	60	6 / 9 (Open Lowrise / Sparsely Built)
SEI	0.75	0.16	5.0	6	19	22	59	6 / 9 (Open Lowrise / Sparsely Built)
PUL	0.74	0.16	5.7	6	20	22	58	6 / 9 (Open Lowrise / Sparsely Built)
CE1	> 0.9	< 0.1	< 1	3	0	1	99	D (Low Plants)
CE3	> 0.9	< 0.1	< 1	3	0	1	99	D (Low Plants)

Table 1 Urban indicators values for the thirteen selected LCZ. SVF: Sky view factor, AR: Aspect ratio, H: Mean building height, R: Terrain roughness class, Built: Built surface fraction, Imper: Impervious surface fraction, Per: Pervious surface fraction. Adapted from (Leconte et al., 2015).

habitants within an area of 270 km^2. This zone demonstrates a semi-basin situation with two plateaus north east and west. Therefore, the elevation of the area varies between 190 and 420 m above sea level. Two water bodies cross the area, namely the Meurthe river and the Marne-Rhine channel. Nancy demonstrates a Cfb climate according to the Köppen-Geiger classification (Peel et al., 2007). Between June and September, the daily air temperature maximum is 23.2℃ and the daily air temperature minimum is 12.2℃ on average over the last 30 years. Over this period, the mean amount of precipitation is 64.8 mm per month.

Local climate zones have been determined for the Great Nancy Area. The process of construction of these LCZ has been organized into three steps. First, the contours of the LCZ have been determined over the area of interest. Mean building height and land use of the zones have been estimated in order to draw these contours. At this point, an estimated LCZ type has been assigned to the each of these areas based on these two information. Second, 13 LCZ have been selected among the LCZ determined in the Great Nancy Area. They have been chosen with similar elevation in order to avoid that the temperature measurements will be impacted by thermal effect due to topography. Seven urban indicators have been calculated within each LCZ of this selection (cf table 1). The sky view factor has been calculated for each pixel of a digital elevation model (DEM) using SAGA GIS (Böhner et al., 2006). Sky view factor value for a given LCZ corresponds to the spatial average of the values within this zone. The aspect ratio has been calculated for each LCZ using the approach described by Masson (2000). Mean building height and building surface fraction have been determined using a national database for

building footprints (BD TOPO©). Terrain roughness class values have been determined according to the Davenport classification. Rules of thumb mentioned by (Grimmond and Oke, 1999) have been used to estimate the roughness length and the displacement height for each LCZ. Impervious and pervious surface fraction have been manually calculated for each LCZ of the selection using visible satellite imagery data. Third, the best match has been found between each of the 13 zones and one of the 17 types of LCZ, based notably on indicators values. The selection of LCZ is composed of three LCZ 2, three LCZ 5, two LCZ 8, three LCZ 6/9 and two LCZ D.

It appears that the identification of the relevant LCZ type for the residential areas has been complex. For JAR, PUL and SEI, the land use indicator values are at the limit between LCZ type 6 and LCZ type 9. Moreover, morphological indicators do not allow to select one of these two types, since sky view factor values are type 6 and aspect ratio values are type 9. Therefore, any choice could have been performed between the LCZ type 6 and the LCZ type 9. Thus, these areas have been considered both Open Lowrise and Sparsely Built for this study. This approach does not affect the processing of the meteorological records since calculations have been identical for all the zones regardless their LCZ type. Complementary information regarding the LCZ building process can be found in (Leconte et al., 2015).

2.2 Hourly mobile measurements

In order to observe in details the nocturnal cooling within the local climate zones of Nancy, air temperature measurements have been performed at hourly basis. The route needed to be carried out in less than 1 h so as to reach a time frequency of one measurement per hour. Therefore, only four LCZs have been chosen among the selection of 13 LCZ : CEN, OUE, THL, and JAR (figure 1). These LCZs are located in the center of the Great Nancy Area.

Measurements have been performed under meteorological conditions that lead to substantial urban heat island amplitude, namely anticyclonic conditions, low wind speed (below 6 $m.s^{-1}$ at 10 m above the ground), cloud cover below or equal to 2 octas, and absence of precipitation during the previous 24 h. Meteorological data regarding wind speed 10 meters above the ground, cloud cover, and precipitation have been gathered from the meteorological station of the Nancy-Essey airfield (WMO Index Number 07180) which is located within a LCZ type D. Meteorological conditions observed on the day of measurements are similar to the conditions of the previous day. Measurements are realized using a PT100 sensor mounted on the roof of a vehicle. This probe has an accuracy of ±0.2℃. In order to investigate the canyon temperature, it is placed at 2 m high inside a ventilated cylinder to avoid dust deposit and droplets on the sensor. Data corresponding to vehicle speed below 15 $km.h^{-1}$ are not considered, in order to avoid thermal perturbations from other vehicles during the stops. Air temperature is recorded every 3 m. The mean air temperature of a given LCZ correspond to the arithmetical average of all the measurement points that are within the contour of the LCZ. The mobile measurements are performed within streets. This may introduce a bias in air temperature records, since areas where the vehicle can not access (e.g. parks, gardens and private spaces) are put aside.

Two measurements sessions have been realized :

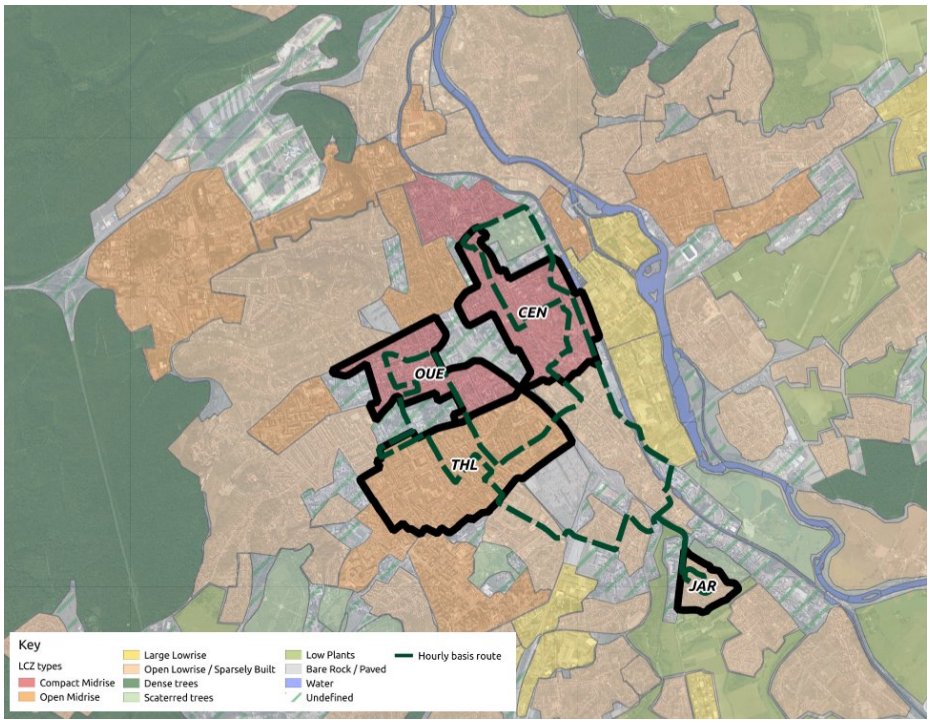

Fig. 1 Measurement route for mobile measurements performed on hourly basis the 2nd August 2013 and the 21st August 2013. The four studied LCZ are underlined in black.

- The 2 August 2013 between 4:30 and 23:30 (local time)
- Between the 21 August 2013 at 8:00 and the 22 August 2013 at 7:30 (local time)

In the following sections, all times are expressed in local time which correspond to UTC+2. In the case of the 2nd of August, cloud cover was below 2 octas during the morning, and then raised suddenly to 6 octas around 17:00. During the rest of the evening, the cloud cover was between 1 and 4 octas.

3 Air temperature dynamics: Observation of a two-phases nocturnal cooling

The air temperature dynamics are observed during the two hourly measurements sessions (2 August 2013 and 21 August 2013). Figures 2 and 3 present air temperature within the four studied LCZs. Each point on the graph corresponds to the spatially averaged air temperature within a given LCZ at a given time (written as $\overline{T_{air}}$). The number of points T_{air} performed during one passing differs between the areas. On average, 300 measurements are carried out in JAR for one passing, 450 for OUE, 650 for THL and 800 for CEN.

These two figures show similar patterns in terms of air temperature dynamics. At sunrise, the four LCZs demonstrate temperature differences (cf. figure 2). Just

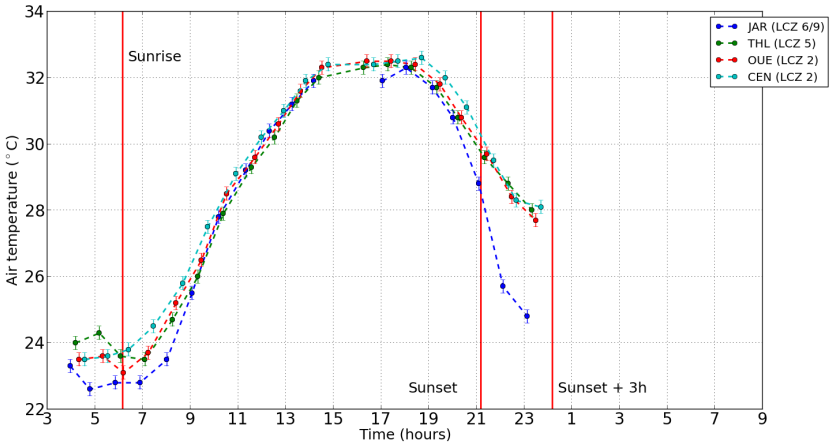

Fig. 2 Air temperature recorded at hourly basis within four LCZ (2nd August 2013). Vertical red lines show sunrise, sunset and 3 hours after sunset. Error bars correspond to global uncertainties.

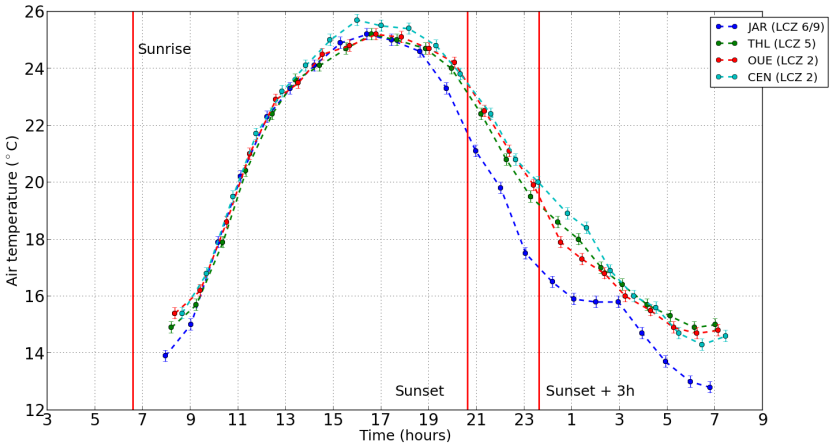

Fig. 3 Air temperature recorded at hourly basis within four LCZ (21st August 2013). Vertical red lines show sunrise, sunset and 3 hours after sunset. Error bars correspond to global uncertainties.

after the sunrise, downward short-wave radiative flux increases, and the air temperature of the four LCZs tend to converge toward a similar value. The four LCZs show very similar air temperature from 3 h after sunrise to approximately 17:00.

About 1 to 2 h before sunset, the downward short-wave radiative flux sharply decreases. At this moment, the air temperature of JAR starts to differ from the other LCZs. Between 1 to 2 h before sunset to 3 to 5 h after sunset, JAR cools down faster than the other LCZs. For the 21 August 2013, the maximal air temperature gap between JAR and the other LCZs is reached approximately 3 h after sunset

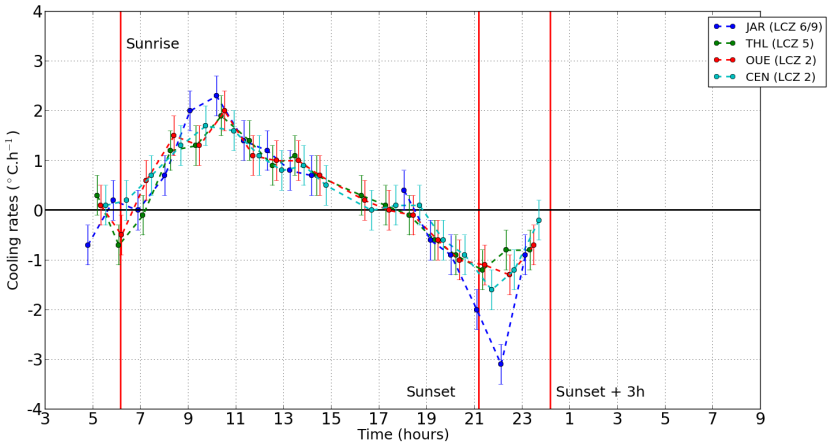

Fig. 4 Hourly cooling rates for the four selected LCZ (2nd August 2013). Vertical red lines show sunrise, sunset and 3 hours after sunset. Error bars correspond to global uncertainties.

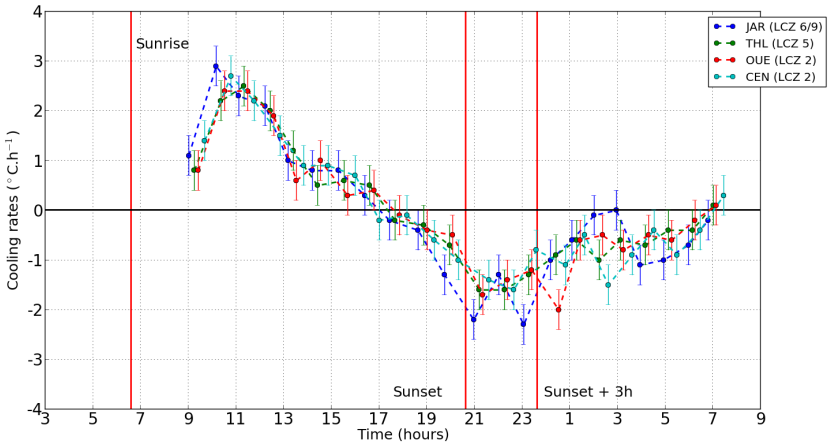

Fig. 5 Hourly cooling rates for the four selected LCZ (21st August 2013). Vertical red lines show sunrise, sunset and 3 hours after sunset. Error bars correspond to global uncertainties.

(around 3℃ between JAR and CEN) (figure 3). Then between 0:00 to 8:00, the air temperature gap between JAR and the other LCZs remains stable. JAR's air temperature gets closer from the temperature of the other LCZs only around 3:00.

Hourly cooling rates are also determined on this data set. For the session of 2 August 2013, cooling rates are close for all the LCZ during the most part of the day (figure 4). Around 20:00, cooling rate values start to diverge. Between 20:00 and 0:00, the mean cooling rate is lower for JAR (-1.7℃.h^{-1}) than for the other LCZ (-0.9℃.h^{-1} for THL, -1℃.h^{-1} for OUE, -1℃.h^{-1} for CEN).

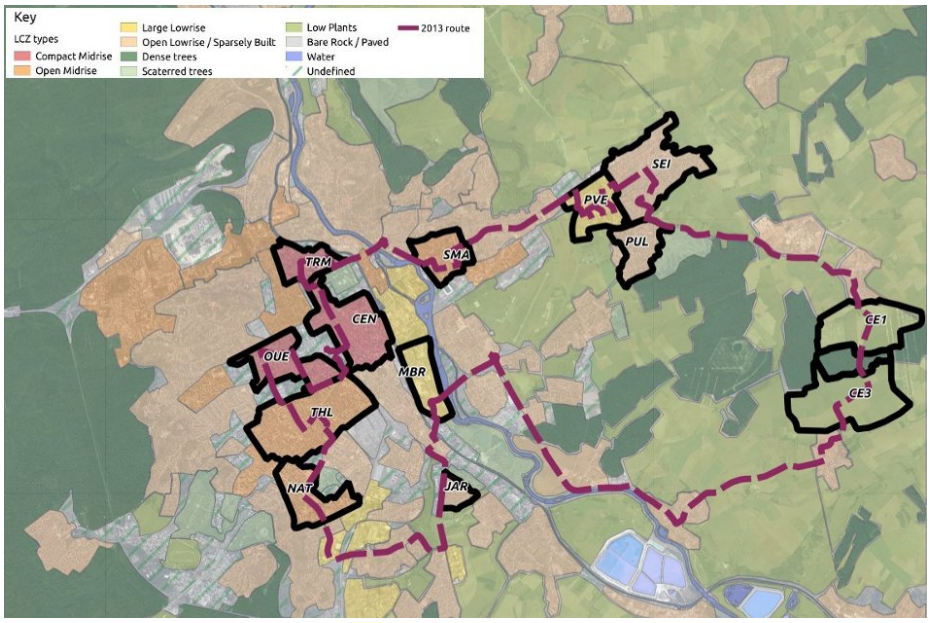

Fig. 6 Measurement route for mobile measurements performed in the conurbation of Nancy during summer 2013. The thirteen studied LCZ are underlined in black. Adapted from (Leconte et al., 2015)

Observations are very similar for the session of 21 August 2013 (figure 5). As for 2 August 2013, cooling rate values are similar between the four LCZs during daytime and only diverge around 20:00. Between 20:00 and 0:00, mean cooling rate for JAR (-1.8℃.h^{-1}) is lower than the mean cooling rates of the other LCZs (-1.3℃.h^{-1} for THL, -1.2℃.h^{-1} for OUE, -1.2℃.h^{-1} for CEN). This difference in terms of cooling rate leads to the maximum temperature gap observed at 0:00. Between 0:00 and 8:00, cooling rate values are similar between the four LCZs : -0.6℃.h^{-1} for JAR, -0.6℃.h^{-1} for THL, -0.6℃.h^{-1} for OUE and -0.7℃.h^{-1} for CEN.

This section highlights that air temperature differences between LCZ are low at the end of the afternoon, and important 3 to 5 h after sunset. Between these two periods, LCZs demonstrate different cooling rates, leading to air temperature gaps between LCZ. For the 21 August 2013 in particular, air temperature records underline the two-phase nocturnal cooling introduced by Holmer et al. (2007).

4 Extension of the two-phase nocturnal cooling framework

4.1 Data set

The two-phase nocturnal cooling framework is extended to a larger meteorological data set which includes a greater number of LCZ so as to corroborate the first observations. In parallel of the hourly measurements sessions, a selection of 13 LCZs has been investigated in 2013 (cf. section 2.1). Sixteen mobile measurements

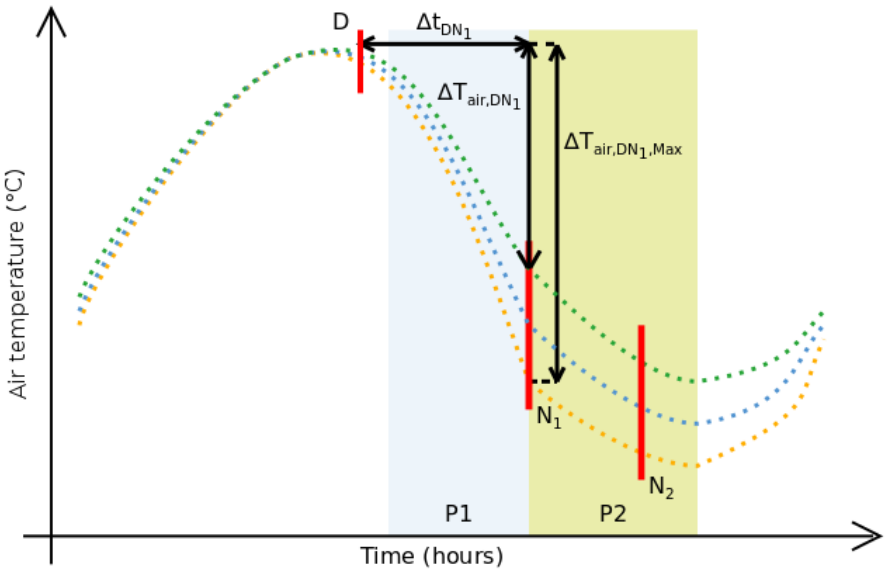

Fig. 7 Theoretical nocturnal cooling phases for three LCZ of different types. Phase 1 (P1, blue area) is between one to three hours before sunset and three to five hours after sunset. Phase 2 (P2, green area) is between three to five hours after sunset and sunrise. The letter D refers to the sessions performed in the middle of the afternoon, letter N_1 refers to the sessions carried out around 3 hours after sunset, letter N_2 refers to the sessions realized around 7 hours after sunset.

have been performed within these areas under similar weather conditions and with the same instrumented vehicle than the experimental setting presented previously. A detailed description of this measurement campaign is provided in (Leconte et al., 2015). The travel time for this itinerary is approximately 2 h 30 min (figure 6), and regional air temperature varies during the measurement session. Therefore, a linear time correction scheme has been applied (Leconte et al., 2015).

4.2 Phase 1

For the extension to phase 1, the selected data set contains only two measurements per day which have been performed during the afternoon and at nighttime. Afternoon session hour is between 14:00 and 17:00, which usually corresponds to the daily maximum air temperature under these specific weather conditions (Oke, 1987). The nighttime session hour is chosen to record the maximum of the urban heat island amplitude (Oke, 1987), i.e. approximately 3 h after sunset, between 0:00 and 3:00.

Figure 7 locates the sessions regarding the theoretical nocturnal cooling phases. For diurnal (resp. nocturnal) sessions, the reference hour is the end of the session (resp. the beginning of the session), therefore the corresponding measurements hour is between 16:00 and 18:00 (resp. between 0:00 and 1:00), represented by a letter D (resp. N_1) on figure 7.

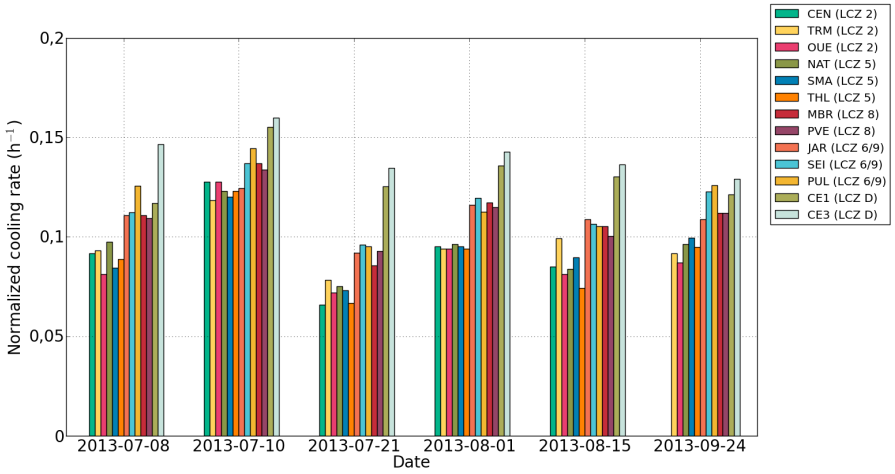

Fig. 8 Normalized cooling rates $\chi^n_{DN_1}$ for the selection of thirteen LCZ for the six studied cases.

To perform the comparison with the hourly measurements, another expression of the cooling rate is proposed. Cooling rates χ_{DN_1} are calculated between session D and session N_1 for each LCZ:

$$\chi_{DN_1} = \frac{\overline{T_{air,D}} - \overline{T_{air,N_1}}}{\Delta t_{DN_1}} = \frac{\Delta T_{air,DN_1}}{\Delta t_{DN_1}} \tag{2}$$

With Δt_{DN_1} the time between session D and session N_1 in hours, $\overline{T_{air,D}}$ the air temperature of a given LCZ at D, $\overline{T_{air,N_1}}$ the air temperature of a given LCZ at N_1. The cooling rate of a LCZ depends on the DTR, however this amplitude varies from one day to another. In order to be able to compare χ_{DN_1} over several days, a climatic indicator which does not vary with DTR is calculated. The proposed normalized cooling rate corresponds to the ratio of the cooling rate over the maximal value of $\Delta T_{air,DN_1}$ (written as $\Delta T_{air,DN_1,max}$). Then, the normalized cooling rate, written as $\chi^n_{DN_1}$, is defined as follows :

$$\chi^n_{DN_1} = \frac{\chi_{DN_1}}{\Delta T_{air,DN_1,max}} \tag{3}$$

Where $\Delta T_{air,DN_1,max}$ is systematically observed for the same LCZ.

In the continuity of the hourly basis measures, 12 measurements sessions (six during daytime, six during nighttime) have been selected. Figure 8 presents $\chi^n_{DN_1}$ values for the 13 selected LCZs. CE3 shows systematically the highest cooling rate. Over this sample, areas of same LCZ type exhibit homogeneous values of $\chi^n_{DN_1}$. Figure 9 highlights that the LCZ types 2 and 5 show the lowest values of $\chi^n_{DN_1}$ of all the LCZ types studied (mean value of 0.093 h^{-1} for both of them). LCZ types 8 and 6/9 demonstrate higher values of $\chi^n_{DN_1}$ than the previous LCZ types (mean value of 0.115 h^{-1} and 0.111 h^{-1} respectively). The highest values of $\chi^n_{DN_1}$ are obtained by the LCZ type D (mean value of 0.136 h^{-1}). It appears that the arrangement of the values of $\chi^n_{DN_1}$ is similar to the six studied cases, except for

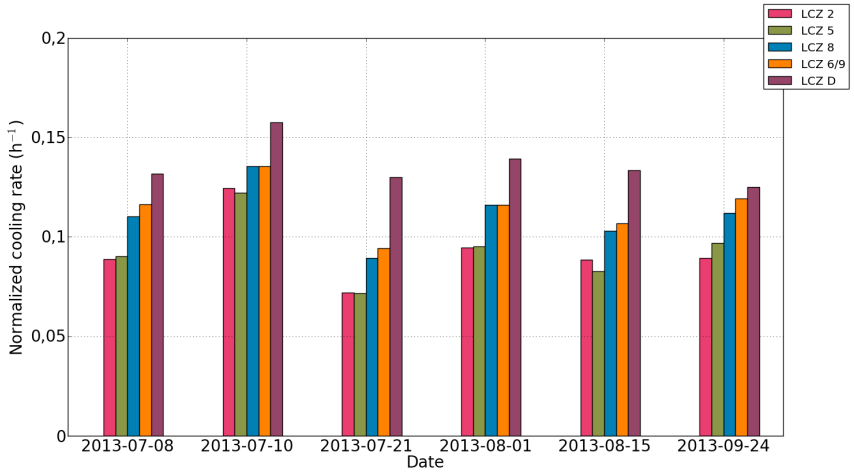

Fig. 9 Normalized cooling rates $\chi^n_{DN_1}$ sorted by LCZ types for the six studied cases.

	LCZ 2	LCZ 5	LCZ 6/9	LCZ 8
LCZ 5	*1.0000*	-	-	-
LCZ 6/9	*0.0003*	*0.0004*	-	-
LCZ 8	*0.0110*	*0.0172*	*1.0000*	-
LCZ D	*<0.0001*	*<0.0001*	*0.0085*	*0.0028*

Table 2 P-values from the Conover-Iman test performed using 77 normalized cooling rate values. Significance level α of *0.05*. The separation between two LCZ types is considered statistically significant if $p - value < \frac{\alpha}{2}$.

the 10 July and 15 August where the values of the LCZ 5 are lower than the values of the LCZ 2. Even if the normalized cooling rates vary over several days for each LCZ type, LCZ types 2 and 5 show systematically lower values that of LCZ types 8 and 6/9, and LCZ type D demonstrates always the highest values.

Statistical tests have been performed in order to assess the statistical significance of the normalized cooling rate values during phase 1. The non-parametric Kruskal-Wallis method has been carried out using 77 normalized cooling rate values organized according to the five studied LCZ types. Results demonstrates that at least one LCZ type has a different statistical distribution than the others ($\chi^2 = 37.5425, p - value < 0.0001$). Then, the Conover-Iman method has been applied as Kruskal-Wallis post hoc so as to analysis the multiple pairwise comparisons. Considering a common significance level α of *0.05*, this test shows a significant separation of all LCZ (i.e. $p - value < \frac{\alpha}{2}$) except between LCZ 2 and LCZ 5 and between LCZ 69 and LCZ 8 (cf. table 2).

4.3 Phase 2

The study of the phase 2 is performed using another data set. Table 3 presents the air temperature difference between LCZ types (written as $\Delta T_{LCZ\ X-Y}$) both at the beginning and at the end of phase 2. Four measurement sessions are displayed,

	3 hours after sunset			7 hours after sunset		
	July 9	Aug. 15	Mean value	Sept. 5	Sept. 6	Mean value
$\Delta T_{LCZ\ 2-D}$	4.7℃	4.1℃	4.4℃	3.9℃	4.6℃	4.3℃
$\Delta T_{LCZ\ 5-D}$	4.4℃	4.1℃	4.3℃	3.3℃	3.6℃	3.5℃
$\Delta T_{LCZ\ 6/9-D}$	3.0℃	3.0℃	3.0℃	2.6℃	2.8℃	2.7℃
$\Delta T_{LCZ\ 8-D}$	2.7℃	2.4℃	2.6℃	2.2℃	2.4℃	2.3℃

Table 3 Average air temperature difference between four LCZ types and the LCZ type Low Plants $\Delta T_{LCZ\ X-D}$. 3 hours after sunset: Cloud cover 0, Mean wind speed at 10 meters : 1.2 m.s^{-1}, 9th July 2013 and 15th August 2013. 7 hours after sunset: Cloud cover 0, Mean wind speed at 10 meters : 0.8 m.s^{-1}, 5th September 2013 and 6th September 2013.

namely two sessions at the beginning of phase 2 – 3 h after sunset, N_1 on figure 7 – and two sessions at the end of phase 2 – 7 h after sunset, N_2 on figure 7. These four measurements have been selected with similar conditions of low cloud cover and low wind speed. Each value of the table corresponds to the difference between the mean air temperature of a given LCZ type and the mean air temperature of LCZ type low plants ($\Delta T_{LCZ\ X-D}$).

Results demonstrate that the air temperature differences observed 3 h after sunset are similar to the one observed 7 h after sunset. Air temperature differences are very similar between N_1 and N_2 for the LCZ types 2, 6/9 and 8 (with a gap of 0.1℃, 0.3℃ and 0.3℃ respectively). The air temperature difference is more important for the LCZ type 5 (0.8℃ between N_1 and N_2). It appears that the air temperature differences remain globally stable during the phase 2. This tends to confirm the observation of the hourly basis measures, namely that air temperature cooling is similar during phase 2 for all the LCZ.

4.4 Influence of relative position of LCZ over normalized cooling rate values

In order to analyze the influence of the relative position of LCZ within the conurbation on the nocturnal cooling dynamics during phase 1, the relationship between the distance to the center of the conurbation and the mean normalized cooling rate differences has been investigated (Figure 10). The normalized cooling rate differences are calculated regarding the mean $\chi^n_{DN_1}$ value of CEN. The distances to the center are expressed regarding CEN which is located approximately at the center of the conurbation. LCZs 2 and 5 demonstrate homogeneous cooling dynamics, corresponding to the lowest values of mean normalized cooling rates differences, e.g. $\pm$ 0.0028 h^{-1}. They are located close to the center of the conurbation, within a perimeter of 3.2 km. LCZs 6/9 and 8 show mean normalized cooling rate differences of the same order of magnitude, between 0.017 h^{-1} and 0.025 h^{-1}. For this group of LCZ, distance to center varies between 1.7 and 6.2 km.

Experimental values highlights that the LCZ type of an urban area is a key factor regarding its nocturnal cooling dynamics. Results show that LCZ that have a similar distance to the center (e.g. 3.2 km for NAT and 3.6 km for JAR) but dissimilar LCZ type have different mean normalized cooling rate differences values (0.0023 h^{-1} for NAT and 0.0171 h^{-1} for JAR). The same observation can be performed between MBR and THL, which demonstrate distances to the center of

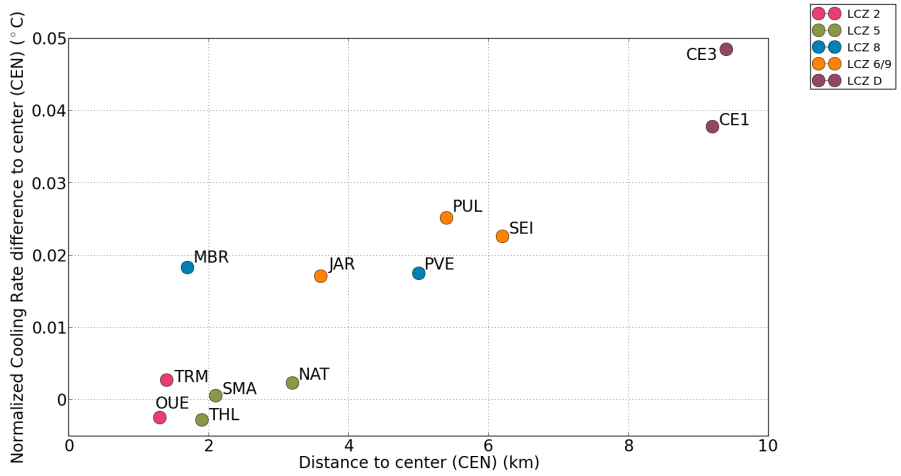

Fig. 10 Mean normalized cooling rate differences as a function of the distance to CEN (LCZ 2), located approximately at the center of the conurbation. Normalized cooling rate differences and distances are expressed relatively to this area. Measurement time is 0:30.

1.7 km and 1.9 km and mean normalized cooling rate differences values of 0.0183 h^{-1} and -0.0028 h^{-1} respectively.

Nonetheless, for LCZ 6/9, the LCZ closest to the center present the lowest mean normalized cooling rates differences values. Indeed, JAR's distance to the center is 3.6 km for a normalized cooling rates differences value of 0.0171 h^{-1}, when SEI and PUL have a higher distance to the center (6.5 and 5.4 km respectively) and higher normalized cooling rates differences value (0.0226 h^{-1} and 0.0251 h^{-1} respectively). Thus, the distance to the center seems to have an influence of nocturnal cooling for this LCZ type.

5 Discussion

Hourly measurements sessions show that the cooling differences between the LCZ leads to the formation of the urban heat island. However, it appears that during phase 1, the thermal behaviors of several LCZ types seems to be similar. This result is highlighted by the Conover-Iman test. Indeed, regarding air temperature dynamics during phase 1, LCZ 2 can be grouped with LCZ 5, and LCZ 8 is similar to LCZ 6/9. Regarding the values of normalized cooling rates, it is possible to build three groups, a groupe "midrise" with the LCZ 2 and 5, a groupe "lowrise" with the LCZ 8 and 6/9, and a group "plant" with the LCZ D. Each of these three groups correspond to a specific thermal behavior (figure 11).

These three groups could be explained regarding the urban features of the studied LCZ types. These areas are characterized by the ten urban indicators that are part of the LCZ classification scheme. Seven urban indicators concerning urban morphology and land use have been calculated for the selection of 13 LCZs. The LCZ types 2 and 5 demonstrate common features in terms of urban morphology: sky view factor is always below 0.7, aspect ratio is above 0.35, mean

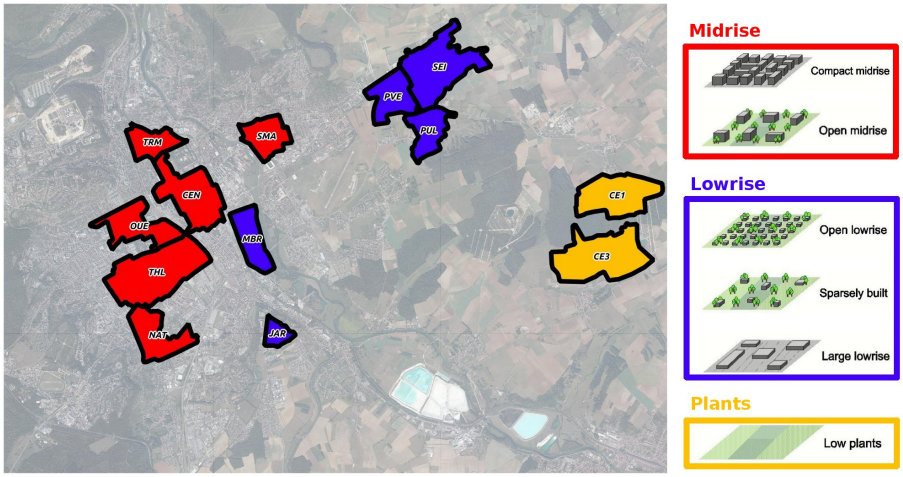

Fig. 11 LCZ groups "Midrise", "Lowrise" and "Plants" based on nocturnal cooling rate values.

	Phase 1	Phase 2
Public square, Göteborg	-1.6°C.h^{-1}	-0.6°C.h^{-1}
Urban canyon, Göteborg	-1.2°C.h^{-1}	-0.6°C.h^{-1}
LCZ 6 / 9 (JAR), Nancy	-1.8°C.h^{-1}	-0.6°C.h^{-1}
LCZ 2 and 5 (CEN, OUE, THL), Nancy	-1.2°C.h^{-1}	-0.6°C.h^{-1}

Table 4 Cooling rates calculated at Göteborg and Nancy. Göteborg data correspond to August and September 1999, Nancy data correspond to the 21st August 2013 (Holmer et al., 2007). For the two cities, values are calculated between one hour before sunset and two hours after sunset for phase 1, and between three hours after sunset and ten hours after sunset for phase 2.

building height is above 10 m and terrain roughness class is 7. Similarly, the urban indicators of the LCZs 8 and 6/9 show similar aspects: sky view factor is always above 0.6, aspect ratio is below 0.2, mean building height is below 10 m and terrain roughness class is 6 or below. In the meantime, any common pattern emerge from the analysis of the land use indicators. Therefore, it seems that for this case study, the urban morphology is a key factor for air temperature dynamics during phase 1, leading to the development of three groups of normalized cooling rates values ("midrise", "lowrise" and "plant"). During this phase, low sky view factor values and important mean building height could lead to a significant modification of the long-wave radiative energy balance and to a decrease of the sensible heat release from the surface. These two phenomenons could be responsible of the distinct nocturnal cooling behaviors between "midrise" group and "lowrise" group, in association with the use of different building material and peculiarities in terms of anthropogenic heat sources.

Recent studies which tackle air temperature dynamics have calculated cooling rates from data set provided by weather station, therefore the corresponding measurements are representative of the area nearby the sensors (named as source area or footprint). Local climate zone have been determined only in Oua-

gadougou (Holmer et al., 2013) in order to define the measurement environments and also to ensure that the sources area for the sensors were large (radius of 400 m) and homogeneous in terms of urban indicators. In his work in Göteborg, Holmer et al. (2007) proposes values of cooling rates calculated from experimental sites located within an homogeneous zone of 300 m. It appears that the results from the Göteborg sites match with the one realized in Nancy (table 4). During phase 1, cooling rate is lower for dense urban morphologies (-1.6℃.h^{-1} for Urban canyon in Göteborg, -1.8℃.h^{-1} for LCZ 2 and 5 in Nancy) than for the open morphologies (-1.2℃.h^{-1} for both Public square in Göteborg and LCZ 6/9 in Nancy). In phase 2, the morphology seems to not impact the cooling rate, which is homogeneous for all areas (-0.6℃.h^{-1}). This comparison demonstrates that results obtained by Holmer et al. (2007) at micro scale (street scale) can be observed at local scale, using simultaneously the Local Climate Zone classification and high density mobile measurements.

Air circulation could be one of the explanation concerning the importance of the parameter "distance to the center" over the nocturnal cooling rate values for LCZ 6/9. Indeed, air from the warmest LCZ located in the center of the conurbation could be advected toward the contiguous LCZ, creating a temperature gap between LCZs that belong to the same LCZ type but have different positions within the city. However, any additional measurements have been performed to validate this hypothesis. This cooling rate difference between the three LCZ 6/9 could also be explained by sampling error or by dissimilar values of urban parameters.

6 Conclusion

This work examines the nocturnal cooling of LCZ involving cooling rate calculations and mobile measurement campaigns. The case study concerns the local climate zones of the conurbation of Nancy, France. The air temperature dynamics of these zones are investigated using an instrumented vehicle. First, two hourly measurements sessions are realized within four LCZ of Nancy. During these two periods, a two-phases nocturnal cooling has been observed. Results highlight that cooling rates during phase 1 vary depending on LCZ types. Second, the observations during hourly measurements are confronted with a larger data set composed by a selection of 13 LCZs. In order to carry out this comparison, a new climatic indicator is proposed for the phase 1. It consists in calculating cooling rates scaled by the maximum value of $\Delta T_{air,DN_1}$. The use of the normalized cooling rate highlights that LCZs 2 and 5 demonstrate analogous air temperature dynamics during phase 1. Similarly, LCZs 8 and 6/9 show close normalized cooling rate values. Urban indicators that characterize district morphology seem to be influential parameters regarding temperature decrease in phase 1. Mean air temperature differences between LCZ tend to remain constant during phase 2, according to the observations of Holmer et al. (2007). Within the conurbation, the LCZ type is a parameter more relevant than the distance to the center. Comparison of results between Göteborg and Nancy shows that cooling rates values are in good agreement. Normalized cooling rate values tend to sort LCZ of Nancy into three groups regarding their air temperature dynamics. Each of these three groups demonstrates a particular range of urban morphological indicators independent from the others.

It appears that the normalized cooling rate is a simple climatic indicator that provides quantitative information about the nocturnal cooling of LCZ, and therefore about the dynamic thermal behavior of neighborhoods. In this study, normalized cooling rate is applied on LCZ scheme, which are areas characterized by ten urban indicators. This combination between a climatic indicator and an urban climate classification is able to highlight the link between the nocturnal cooling of a neighborhood and its urban features.

Acknowledgements This work has been supported by the French Environment and Energy Management Agency (ADEME) and the GEMCEA.

References

P. Alexander and G. Mills. Local Climate Classification and Dublin's Urban Heat Island. *Atmosphere*, 5:755–774, 2014.

P.J. Alexander, G. Mills, and R. Fealy. Using LCZ data to run an urban energy balance model. *Urban Climate*, 13:14–37, 2015.

B. Bechtel, P. Alexander, J. Böhner, J. Ching, O. Conrad, J. Feddema, G. Mills, L. See, and I. Stewart. Mapping Local Climate Zones for a worldwide database of the form and function of cities. *ISPRS International Journal of Geo-information*, 4:199–219, 2015.

J. Böhner, K.R. McCloy, and J. Strobl. *SAGA - Analysis and Modeling Applications*. Göttinger Geographische Abhanlungen, 2006.

W.T.L. Chow and M. Roth. Temporal dynamics of the urban heat island of Singapore. *International Journal of Climatology*, 26:2243–2260, 2006.

R. Ellefsen. Mapping and measuring buildings in the urban canopy boundary layer in ten US cities. *Energy and Buildings*, 15-16:1025–1049, 1990/1991.

R. Emmanuel and E. Krüger. Urban heat island and its impact on climate change resilience in a shrinking city: The case of Glasgow, UK. *Building and Environment*, 53:137–149, 2012.

E. Erell and T. Williamson. Intra-urban differences in canopy layer air temperature at a mid-latitude city. *International Journal of Climatology*, 27:1243–1255, 2007.

E. Erell, D. Pearlmutter, and T. Williamson. *Urban microclimate : designing the spaces between buildings*. Earthscan, 2011.

D. Fenner, F. Meier, D. Scherer, and A. Polse. Spatial and temporal air temperature variability in Berlin, Germany, during the years 2001-2010. *Urban Climate*, 10:308–331, 2014.

L. Gartland. *Heat Island : Understanding and Mitigating Heat in Urban Areas*. Earthscan, 2008.

K. Giannopoulou, M. Santamouris, I. Livada, C. Georgakis, and Y. Caouris. The impact of canyon geometry on intra urban and urban suburban night temperature differences under warm weather conditions. *Pure and Applied Geophysics*, 167:1433–1449, 2010.

C.S.B. Grimmond and T.R. Oke. Aerodynamic properties of urban areas derived from analysis of surface form. *Journal of Applied Meteorology*, 38:1262–1292, 1999.

M. Haeger-Eugensson and B. Holmer. Advection caused by the urban heat island circulation as a regulating factor on the nocturnal urban heat island. *International Journal of Climatology*, 19:975–988, 1999.

B. Holmer, S. Thorsson, and I. Eliasson. Colling rates, sky view factors and the development of intra-urban air temperature differences. *Geografiska Annaler Series A - Physical Geography*, 89:237–248, 2007.

B. Holmer, S. Thorsson, and J. Lindén. Evening evapotranspirative cooling in relation to vegetation and urban geometry in the city of Ouagadougou, Burkina Faso. *International Journal of Climatology*, 33:3089–3105, 2013.

F. Leconte, J. Bouyer, R. Claverie, and M. Pétrissans. Using Local Climate Zone scheme for UHI assessment: evaluation of the method using mobile measurements. *Building and Environment*, 83:39–49, 2015.

S.-H. Lee and J.-J. Baik. Statistical and dynamical characteristics of the urban heat island intensity in Seoul. *Theoretical and Applied Climatology*, 100:227–237, 2010.

E. Lelovics, J. Unger, T. Gál, and C.V. Gál. Design of an urban monitoring network based on Local Climate Zone mapping and temperature pattern modelling. *Climate Research*, 60:51–62, 2014.

V. Masson. A physically-based scheme for the urban energy budget in atmospheric models. *Boundary-Layer Meteorology*, 94:357–397, 2000.

T. Oke. Toward better scientific communication in urban climate. *Theoretical and Applied Climatology*, 84:179–190, 2006.

T.R. Oke. *Boundary Layer Climate*. Routledge, second edition, 1987.

M.C. Peel, B.L. Finlayson, and T.A. McMahon. Updated world map of the Köppen-Geiger climate classification. *Hydrology and Earth System Sciences*, 11:1633–1644, 2007.

K. Runnalls and T. Oke. Dynamics and controls of the near-surface heat island of Vancouver, British Columbia. *Physical Geography*, 21:283–304, 2000.

I. Stewart and T.R. Oke. Local Climate Zones for urban temperature studies. *Bulletin of American Meteorology Society*, 93:1879–1900, 2012.

N. Theeuwes, G.-J. Steeneveld, R. Ronda, M. Rotach, and A. Holtslag. Cool city mornings by urban heat. *Environmental Research Letters*, 10:114022, 2015.

H. Upmanis, I. Eliasson, and S. Lindqvist. The influence of the green areas on nocturnal temperatures in a high latitude city (Göteborg, Sweden). *International Journal of Climatology*, 18:681–700, 1998.